We are IntechOpen,
the world's leading publisher of
Open Access books
Built by scientists, for scientists

4,800
Open access books available

122,000
International authors and editors

135M
Downloads

154
Countries delivered to

Our authors are among the

TOP 1%
most cited scientists

12.2%
Contributors from top 500 universities

CLARIVATE ANALYTICS

BOOK CITATION INDEX

INDEXED

WEB OF SCIENCE™

Selection of our books indexed in the Book Citation Index
in Web of Science™ Core Collection (BKCI)

Interested in publishing with us?
Contact book.department@intechopen.com

Numbers displayed above are based on latest data collected.
For more information visit www.intechopen.com

Scaling Index Method (SIM): A Novel Technique for Assessment of Local Topological Properties of Porous and Irregular Structures

Irina Sidorenko[1], Roberto Monetti[1], Jan Bauer[2],
Dirk Müller[2] and Christoph Räth[1]
[1]Max-Planck-Institut fuer extraterrestrische Physik
[2]Department of Radiology, Technische Universitaet Muenchen
Germany

1. Introduction

The development of high-resolution visualisation techniques, such as magnetic resonance (MR) and computer tomography (CT) opens the possibility for non-destructive studies of the inner structure of the objects of different nature and origin. The deterioration of the structure with time, deformations and loss of strength under the load and other processes lead to morphological and topological changes inside materials, which require both qualitative analysis and quantitative evaluation. Assessment and proper description of the topological and morphological characteristics of materials with porous and irregular architecture is of great importance for many scientific and engineering studies.

The Scaling Index Method (SIM) is a novel numerical tool for characterising the local topology of an arbitrary structure. By evaluating the local dimensionality of each point, the SIM indicates topologically different substructures: unstructured background, one-dimensional (rod-like) and two-dimensional (plate-like) elements. By changing the parameters of the SIM one can distinguish the outer surface from inner points of the structure, describe structures at different scales, and include anisotropic features of the tissue. This method can be applied to both binary and greyscale multidimensional images. To demonstrate the scientific performance of the method we apply numerical techniques based on the SIM to tree-dimensional μCT images of the bone tissue engineering scaffolds (as an example of designed porous structure) and to trabecular bone specimens taken from the human vertebrae in vitro (as an example of biological tissue with very irregular and complicated structure). A proper description of the global and local structural characteristics of the trabecular bone network, which carries and redistributes mechanical load inside the bone, helps to evaluate the deterioration of bone tissue caused by osteoporosis and to predict the most frequent complications of this disease, namely spine and hip fractures. Because of the porous and very irregular architecture of the trabecular bone tissue, a detailed assessment of such a structure requires the use of many texture measures derived from different morphological, biomechanical, topological, and statistical concepts. We show that the Scaling Index Method provides complementary information to the existing well-established techniques.

One of the most frequently used morphological parameter in classical three-dimensional morphometric analysis is the Structure Model Index (*SMI*). It quantifies the type of the structure by the estimation of the plate-to-rode ratio, which is calculated by means of three-dimensional differential analysis of the triangulated bone surface. Scaling Index Method proposes a new approach for the calculation of rode-plate ratio, leading to the novel approach of calculation *SMI*. Combination of the SIM, which describes the topology of the structure on a local level, with Finite Element Method (FEM), which models the biomechanical behaviour of the bone, gives a possibility to analyse redistribution of the stresses and deformations within topologically different structure elements. Minkowski Functionals (MF) supply global morphological information about any structure. According to integral geometry the topology of an arbitrary 3D body can be described by four quantities, known as the Minkowski Functionals, which represent the volume (MF_1), the surface (MF_2), the integral mean curvature (MF_3), and connectivity number (MF_4). The first and second Minkowski Functionals (MF_1 and MF_2) correspond to the bone volume fraction *BV/TV* and normalized bone surface area *BS/TV*, respectively. To extract global morphological characteristics of the trabecular structure, Minkowski Functionals are calculated from the binarized high-resolution image. In conventional approach binarization is made according to the grey level value. In our study we threshold 3D μCT images according to the local structure characteristic calculated by SIM. Such a nonlinear combination of the SIM and MF opens a possibility to calculate *global* topological properties for substructures selected according to their *local* topology.

We provide a detailed theoretical description of the Scaling Index Method with examples of its application in the second section. In the third section we demonstrate possible combinations of SIM with existing numerical techniques and compare the diagnostic performance of the numerical methods and their combinations with SIM by Pearson's correlation analysis with respect to the maximum compressive strength (MCS) measured in biomechanical tests. In the fourth section we summarize main conclusions and underline advantages and perspectives of the proposed Scaling Index Method.

2. Scaling Index Method (SIM)

The Scaling Index Method (SIM) characterises patterns of multi-dimensional point distributions by assessing local topological properties of the underlying structure. The method originated from the study of fractal measures of turbulent and chaotic systems (Benzi et al., 1984), onset of chaos (Jensen et al., 1985), scaling laws for chaotic attractors (Paladin & Vulpiani, 1987) and other multifractal objects (Grassberger et al., 1988). With the development of high-resolution image processing Scaling Index Method became an effective tool for analysis of different systems and structures in which nonlinear correlation plays an important role. It was successfully applied to texture detection and discrimination (Räth & Morfil, 1997), cosmological large-scale structures analysis (Räth et al., 2002), fluctuations in the cosmic microwave background (Rossmanith et al., 2009) and trabecular bone network assessment in the context of osteoporosis (Monetti et al., 2003, 2007; Mueller et al., 2006).

2.1 Theoretical background

In SIM a 3D binary image is described as a set of points $\vec{p}_i$ with spatial coordinates *x, y, z*:

$$I(x,y,z) = \{\vec{p}_i\}, i = 1,...,N_{voxels}.$$ (1)

In a 3D greyscale CT or MR image a discrete grey value $g_i(x_i, y_i, z_i)$ of each voxel plays the role of a fourth dimension. Thus, both space and intensity information are combined in a 4D space vector and the image can be regarded as a set of points $\vec{p}_i(x_i, y_i, z_i, g_i)$ in a virtual 4D space. For each point $\vec{p}_i$ we estimate the number of points of the structure in the vicinity with radius r, which determines the length scale on which the structure is analysed. We assume a power law behaviour for the cumulative point distribution function ρ

$$\rho(\vec{p}_i, r) \propto r^{\alpha_i(r)} \tag{2}$$

with exponent $\alpha(r)$, which is called scaling index and has the meaning of a dimensionality of the object. For ordinary shapes like one-dimensional lines and two-dimensional surfaces scaling index α coincides with the usual topological dimension. By varying the scaling radius r one can characterise the same object with different scaling indices α.

In the analysis of nonuniform structures and tissues scaling exponent varies from point to point and it is meaningful to consider pointwise scaling measure, which can be defined as the logarithmic derivative of ρ

$$\alpha_i(r) = \frac{\partial \log \rho(\vec{p}_i, r)}{\partial \log r} = \frac{r}{\rho} \frac{\partial \rho(\vec{p}_i, r)}{\partial r} . \tag{3}$$

In order to calculate scaling indices α one needs to define the number of points within a multidimensional ball with radius r and centre $\vec{p}_i$, i.e. to determine the cumulative point distribution ρ. In principle, any differentiable function and any distance measure between two points can be used for calculation of scaling indices α. In our applications we assume a Gaussian shaping function to weight the cumulative point distribution

$$\rho(\vec{p}_i, r) = \sum_{j=1}^{N} e^{-(d_{ij}/r)2} , \tag{4}$$

where d_{ij} indicates a distance measure between two points in the multidimensional space (3D in case of binary image, or 4D in case of greyscale image). Because of the exponential form of the function ρ the impact of each point is weighted according to its distance d_{ij} from the central point $\vec{p}_i$. This causes SIM to be a local method: the value of the scaling index depends on the number of neighbours in a small vicinity of radius r of the point for which α is calculated, while contributions of points with $d_{ij} > r$ are negligible. For the case of isotropic scaling indices we use the Euclidean distance between two points

$$d_{ij} = \left\| \vec{p}_i - \vec{p}_j \right\|_2 = \sqrt{(x_i - x_j)^2 + (y_i - y_j)^2 + (z_i - z_j)^2} . \tag{5}$$

Anisotropic features of the tissue can be taken into account by using a generalized quadratic distance measure of the form

$$d_{ij} = \sqrt{\lambda_x (x_i - x_j)^2 + \lambda_y (y_i - y_j)^2 + \lambda_z (z_i - z_j)^2} , \tag{6}$$

where λ_x, λ_y, λ_z are the weighting factors of the tree orthogonal spatial directions, respectively. In the case of human vertebrae with natural vertical loading along z-axis we set

$\lambda_x = \lambda_y = 5$ $\lambda_z = 1$. The Scaling Index Method is well suited for quantifying topological aspects on a local level, especially to discriminate substructures with different dimensionality: values of $\alpha \approx 1$ correspond to rod-like components, $1.5 < \alpha < 2.5$ correspond to sheet-like substructure and $\alpha \approx 3$ describe tree-dimensional elements. By means of the SIM a topological characteristic is assigned to each point of the structure, which describes dimensionality of the local neighbourhood. In order to evaluate global topological features based on the local representation of the structure the values of scaling indices can be compiled into the probability density function (pdf)

$$P(\alpha) = prob\left(\alpha \in [\alpha, \alpha + \Delta\alpha]\right). \tag{7}$$

Combining all points of the structure with the same value of scaling index α one obtains structural decomposition of the object according to the local dimensionality of each point.

2.2 Bone tissue engineering scaffolds

One of the most essential features of the Scaling Index Method is its possibility to vary the length scale of the topological decomposition. We demonstrate the scaling flexibility of the SIM by applying to bone engineering scaffolds (Kerckhofs, 2008, 2010), which are examples of designed porous structures. Evaluation of the morphology, mechanical behaviour, material erosion and structural deterioration of such objects is of great importance for many applications in biology, medicine, pharmacy, engineering and other sciences. Regular architecture of the scaffolds gives us exact knowledge of the strut thickness, which we use as a base length for the choice of scaling radius r. For numerical calculations we use μCT images of scaffolds with a resolution of 14 μm. The scaffolds have a strut thickness of 178 μm on average, what corresponds to 12 - 13 pixels length (Fig. 1).
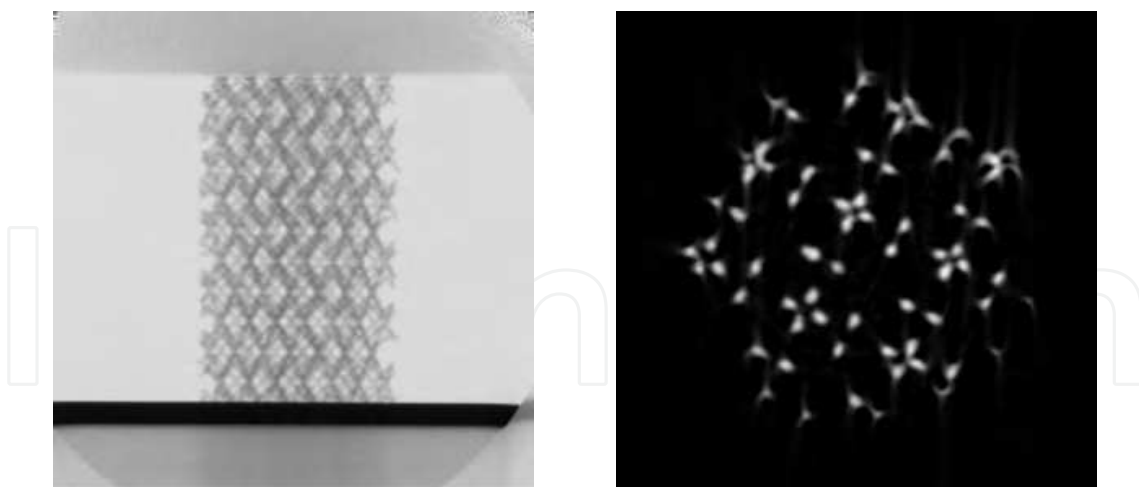

Fig. 1. Original μCT images of the bone engineering scaffolds. Left: side view; right: top view.

In Table 1 we show results of two calculations: with scaling radius $r = 12$ pixels and $r = 2$ pixels. When the scaling radius is comparable with the strut thickness ($r = 12$ pixels, second column of Table 1), all pixels except nodes have $\alpha \in [1,2]$ (blue and green colours), i.e. cylindrical struts are recognised as "thick" one-dimensional elements and the probability distribution function $P(\alpha)$ reaches its maximum at $\alpha \approx 1.7$. When the scaling radius is much
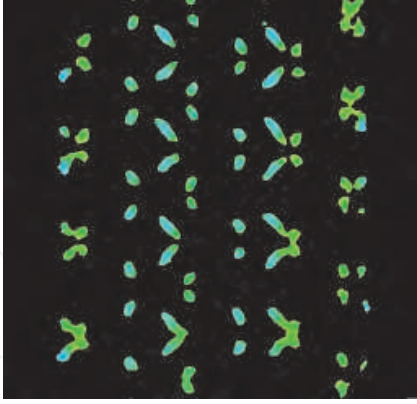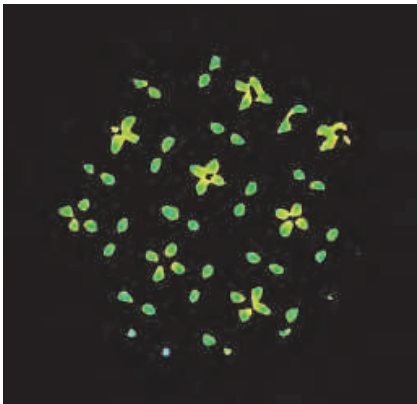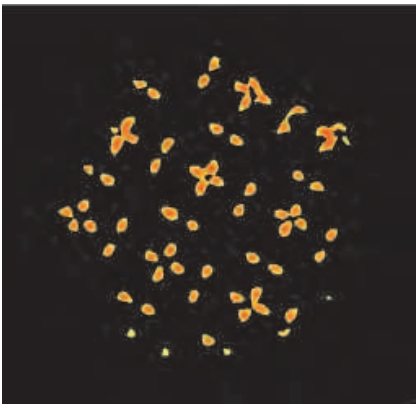
Scaling Index Method (SIM): A Novel Technique for
Assessment of Local Topological Properties of Porous and Irregular Structures

279
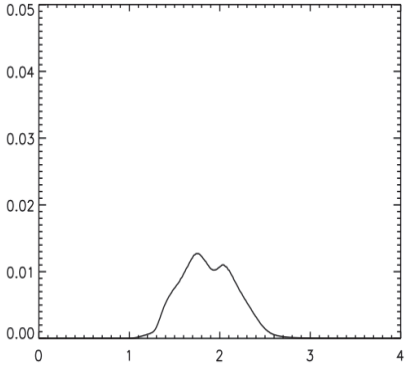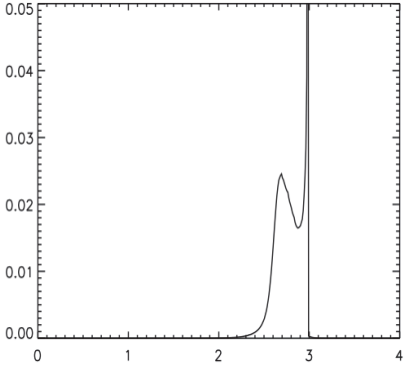
Cross section $y=y_{max}/2$		
Cross section $z=z_{max}/2$		
Probability distribution function $P(\alpha)$		
Parameters of computations	*Scaling radius: r=12 pixels;* *CPU time: 14 hours;* *P(α) mean=1.88;*	*Scaling radius: r=2 pixels;* *CPU time: 12min;* *P(α) mean=2.80;*

Table 1. Scaling index representation of the bone tissue engineering scaffolds. Colour coding: blue *1 < α < 1.5*, green *1.5 < α < 2*, yellow *2 < α <2.5*, red *2.5 < α < 3*.

smaller than the average strut thickness ($r = 2$ pixels, third column of Table 1), SIM provides a very good decomposition of structure elements on the surface and inner body voxels: all inner strut voxels have $\alpha \approx 3$ (red colour on images and the largest peak on the $P(\alpha)$ curve) and surface voxels have $\alpha \approx 2.6$ (yellow colour on images and second large peak on the $P(\alpha)$ curve). Such a α-decomposition can be used in studies of surface erosion, structure deformation under mechanical loading and other applications.

2.3 Trabecular bone

Different biological tissues with irregular structure are the most challenging objects for topological description. In our present paper we use specimens of cancellous bone as a typical example of such a tissue. We base our numerical analysis on 151 µCT images of trabecular network taken from the human vertebrae as previously described in Räth et al., 2008. The scans were acquired for the central 6 mm in length of the specimen using a µCT scanner (Scanco Medical, Bassersdorf, Switzerland). The resulting µCT grey-value images with isotropic spatial resolution of 26 µm were segmented using a fixed global threshold equal to 22% of the maximal grey value to extract the mineralised bone phase. After scanning the 12 mm bone samples were tested by uniaxial compressive experiment and maximum compressive strength (MCS) was determined as the first local maximum of the force-displacement curve. The value of the MCS was used in correlation analysis to assess the diagnostic performance of different numerical methods and their combinations.
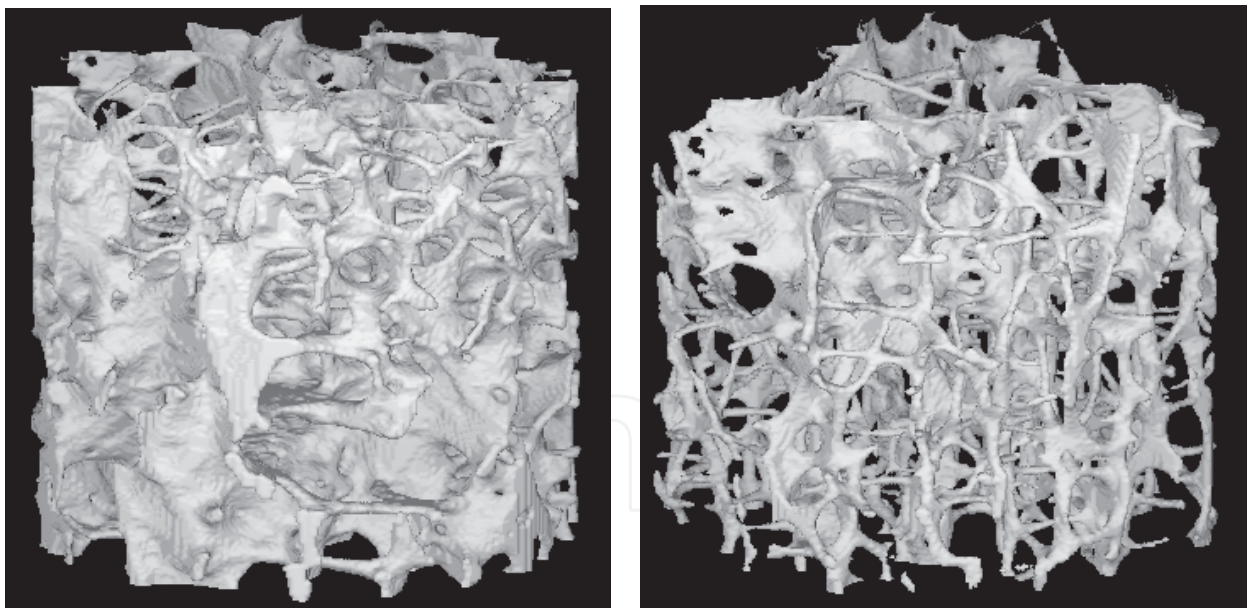

Fig. 2. Original µCT images of the trabecular bone specimens taken from the human vertebrae. Left: strong bone with *BV/TV=0.17* and *MCS=157.00 N*; right: weak bone with *BV/TV=0.07* and *MCS=17.87 N*.

The topological structure of the trabecular network is different for every specimen and reflects its biomechanical features. Typical characteristics of the strong bone (left image on Fig. 2) are following: large amount of plate-like structures, high values of bone mineral content (described by BV/TV) and large fracture load in biomechanical test (described by

MCS). Weak bone (right image on the Fig. 2) has rarefied trabecular network with a lot of rod-like trabecular elements and very small amount of plates, which consequently reflects in low bone mass and fracture load. We apply the Scaling Index Method both with isotropic and anisotropic distance measures d_{ij}, using scale radius r comparable to the average trabecular thickness. For anisotropic SIM we choose the natural direction of vertical loading of human vertebrae (in our notations z-coordinate) as a preferential direction. Analysing the $P(\alpha)$ spectrum of the trabecular structure (Fig. 3) one can distinguish between strong (green curve) and weak (red curve) bones. For specimens with strong trabecular structure the position of the maximum of the $P(\alpha)$ distribution is typically shifted to higher values of α. This systematic shift reflects the fact that strong bones have more plate-like structures and weak bones consist mainly of rod-like elements. This shift in $P(\alpha)$ spectrum is observed both for isotropic and anisotropic SIM and can be used as a structure texture measure for differentiation between strong and weak bones. The additional advantage of the anisotropic approach is the possibility to describe structures in different directions. From the anisotropic $P(\alpha_z)$ spectrum (right plot on Fig. 3) one can conclude that strong bone (green curve) has much more plates along z direction (the largest peak around $\alpha \approx 2.8$) than on the horizontal plane (second maximum around $2 < \alpha < 2.2$). The weaker bone (red curve) has a large amount of horizontal plates, but less vertically elongated plates.
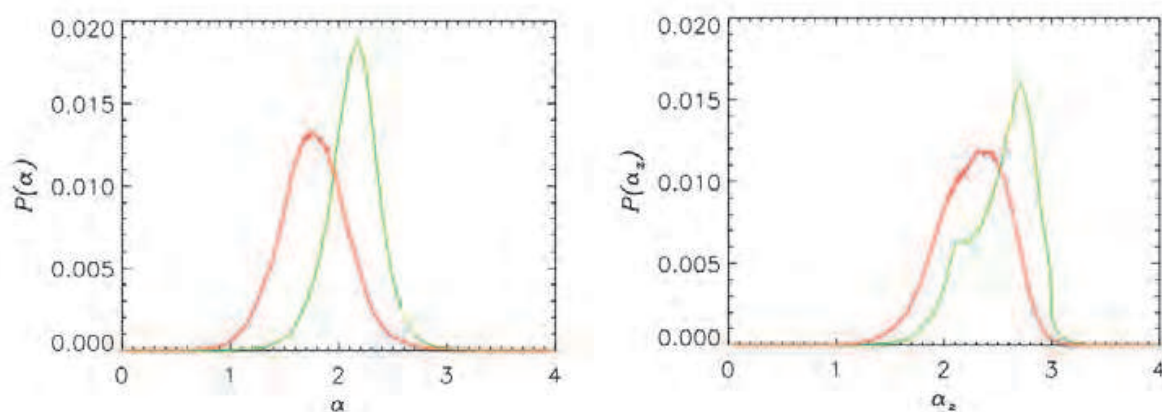

Fig. 3. Probability distribution function of isotropic (left) and anisotropic (right) scaling indices for strong (green curves) and weak (red curves) bones.

The Scaling Index Method provides very clear topological decomposition of the irregular porous structure. Combining all voxels with $\alpha_z < \alpha_{th}$ (Fig. 4) or $\alpha_z > \alpha_{th}$ (Fig. 5) we choose substructures with special topological characteristics and compare trabecular bone elements with different dimensionality. Starting with the small threshold value $\alpha_{th} = 1.7$ we select thin rod-like trabecular elements (first row of Fig. 4). Most of them are horizontally oriented and work for stability of the structure. Increasing threshold value up to $\alpha_{th} = 2$ we can observe all rod-like trabecular elements with any thickness (second row of Fig. 4). By slight increase of threshold value over 2 ($\alpha_{th} > 2.2$, third row in Fig. 4) we add thin horizontal plates into consideration.
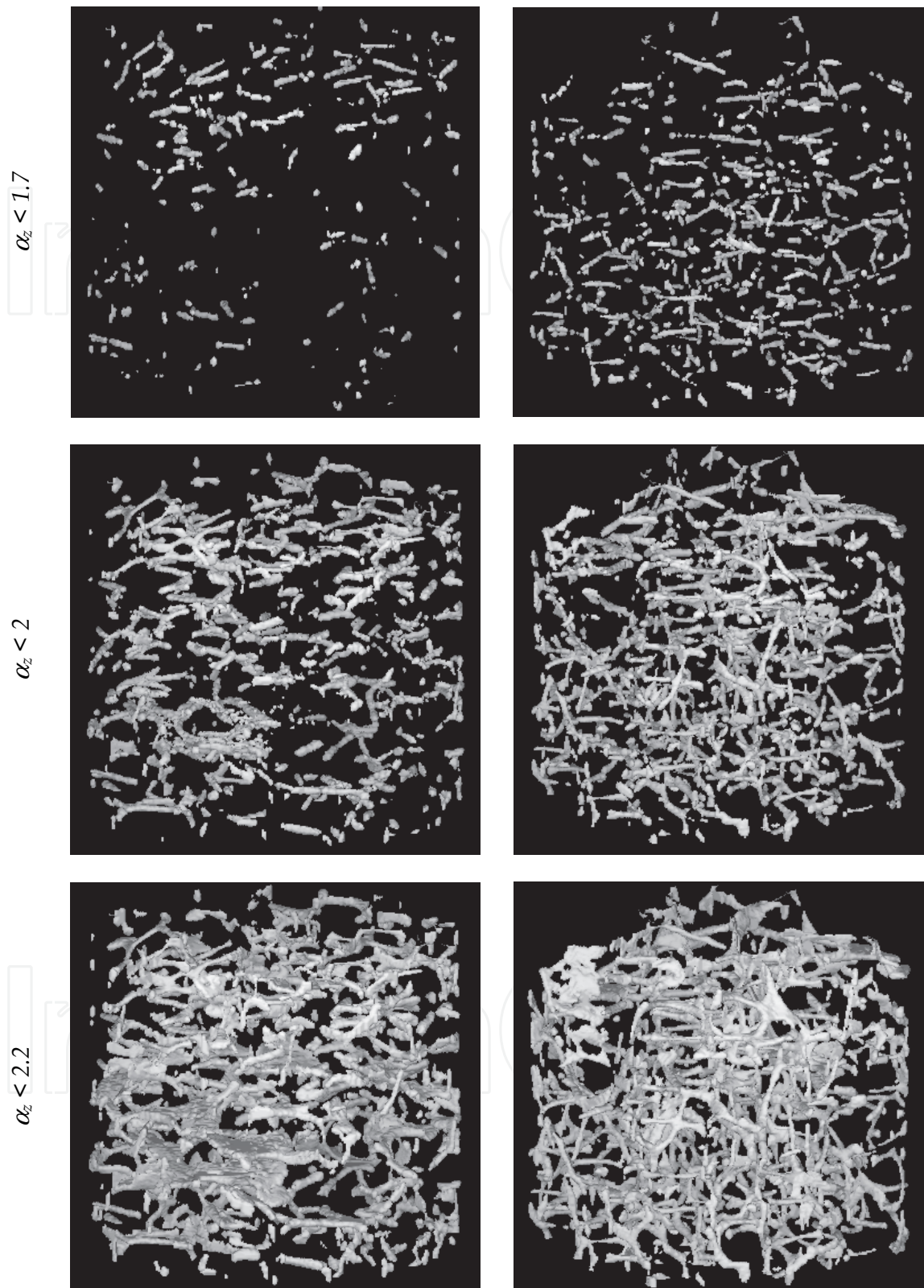
Fig. 4. Topological decomposition of the trabecular bone structure based on the anisotropic scaling index α_z. Substructures are described by voxels with $\alpha_z < \alpha_{th}$. Left: strong bone with *BV/TV=0.17* and *MCS=157.00 N*; right: weak bone with *BV/TV=0.07* and *MCS=17.87 N*.

Scaling Index Method (SIM): A Novel Technique for
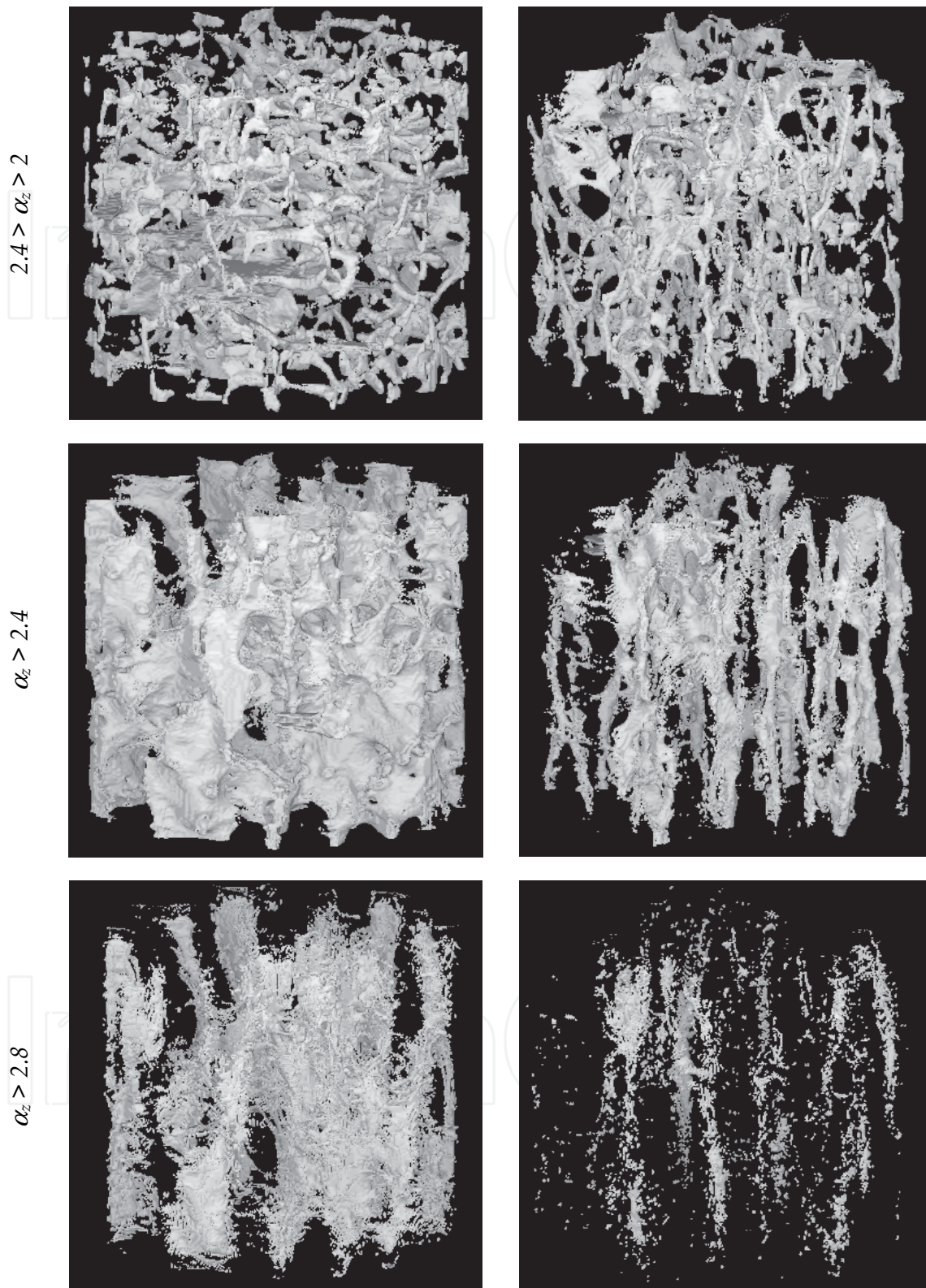Assessment of Local Topological Properties of Porous and Irregular Structures

283

Fig. 5. Topological decomposition of the trabecular bone structure based on the anisotropic scaling index α_z. Substructures are described by voxels with $\alpha_z > \alpha_{th}$. Left: strong bone with *BV/TV=0.17* and *MCS=157.00 N*; right: weak bone with *BV/TV=0.07* and *MCS=17.87 N*.

Assessment of the plate-like structure can be done by choosing all voxels with $\alpha_z > \alpha_{th}$ (Fig. 5). By taking $2 < \alpha_z < 2.4$ we extract thin plate elements (first row in Fig. 5) and by increasing threshold we get more massive, almost three dimensional plates (second and third rows in Fig. 5). Comparison of the vertebrae specimens based on the topological decomposition of the trabecular structure demonstrates several differences in microarchitecture of the strong and weak bones. The microstructure of strong bones has less strut elements and more plates. Both strength and stability are provided by plate-like elements. Thick plates in direction of natural loading (left image of third row in Fig. 5) are main load bearing elements of the structure, while thin horizontal plates (left image of first row in Fig. 5) are responsible for stability of the bone. The trabecular network of weak bones consists of a large amount of rod-like elements oriented in all directions (right column in Fig. 4) and thin plate-like trabecular elements (right column in Fig. 5). Strength of the weak rarefied bones is ensured by both rod- and plate-like elements oriented along natural loading of the structure, while stability of the structure is provided by horizontal thin struts.

3. Combination of the SIM with different numerical methods

Structure analysis of the tissues with porous and irregular architecture is a very complicated task, which requires the application of a large variety of mathematical concepts. In the present section we show that the Scaling Index Method provides complementary information to the existing morphological and biomechanical methods. As an example, we demonstrate that including local topological characteristics into the analysis of the microarchitecture of the cancellous bone, improves qualitative understanding and quantitative evaluation of the trabecular network strength. We assess the diagnostic performance of the numerical techniques by means of Pearson's correlation analysis with respect to the maximum compressive strength (MCS) obtained in biomechanical experiments.

3.1 Morphometric parameters

Morphometric parameters are an efficient numerical tools, which are widely implemented in the standard software delivered by the μCT scanner manufacture. They are determined from the 3D binary images by direct evaluation of typical mean space distances without assumptions of the particular structure model type (Hildebrand & Rüegsegger, 1997a; Hildebrand et al., 1999). Mean Trabecular Thickness (*Tb.Th.*) and mean Trabecular Separation (*Tb.Sp.*) are calculated by filling maximal spheres into the bone mineral tissue or bone marrow, respectively. Trabecular Number (*Tb.N.*) is defined as the number of plates per unit length and can be obtained as the inverse of mean distance between the mid-axes of the structure. Another important morphometric parameter is the Structure Model Index (*SMI*) (Hilderbrand & Rüegsegger, 1997b; Hildebrand et al., 1999; Ding & Hvid, 2000):

$$SMI = 12 \cdot \frac{\varepsilon + \varepsilon^2}{1 + 4(\varepsilon + \varepsilon^2)} \, . \tag{8}$$

The *SMI* characterises the observed structure by estimating the plate-to-rode ratio ε, which is calculated by means of differential analysis of the triangulated bone surface.

In this work we implement a new approach for the estimation of the relative amount of plates to rods. We use the topological decomposition of the trabecular network based on the

Scaling Index Method (SIM): A Novel Technique for
Assessment of Local Topological Properties of Porous and Irregular Structures

285

scaling indices described in section 2.3. For the threshold value of the scaling indices α_{th} we define rods and plates as voxels with $\alpha < \alpha_{th}$ and $\alpha > \alpha_{th}$, respectively. Plate-to-rod ratio is then defined as:

$$\varepsilon = \frac{\sum_{i=1}^{N_{voxels}} H(\alpha_i - \alpha_{th})}{\sum_{i=1}^{N_{voxels}} H(\alpha_{th} - \alpha_i)}. \qquad (9)$$

Here N_{voxels} is number of voxels composing the observed structure and $H(x)$ is the Heaviside step function:

$$H(x) = \begin{cases} 0, & x < 0 \\ 1, & x \geq 0 \end{cases}. \qquad (10)$$

Calculating plate-to-rod ratio ε for different threshold value α_{th} we obtain novel parameters $SMI\alpha$ and $SMI\alpha_z$ as function of α_{th}.

Pearson's correlation analysis with respect to the experimental MCS demonstrates (Table 2) that among classical morphometric parameters the best correlation coefficient $|r_p| = 0.43$ is shown by *Tr.N.* and *SMI*. By the novel nonlinear combination of *SMI* and scaling indices α or α_z we can significantly improve prediction of bone strength and achieve a much higher value of the correlation coefficient: $r_p = -0.74$. The observed improvement in diagnostic performance can be explained by the fact that we combine local topological and global morphometric characteristics in one parameter (*SMI*α or *SMI*α_z in Table 2).

Tb.Th.	Tb.Sp.	Tr.N.	SMI	SMIα	SMIα_z
0.3	-0.41	0.43	-0.43	-0.73	-0.74

Table 2. Pearson's correlation coefficient r_p for classical morphometric parameters and novel combination of *SMI* with isotropic (*SMI*α) and anisotropic (*SMI*α_z) Scaling Index Method.

Analysing $r_p(\alpha_{th})$ curves for the novel parameters $SMI\alpha$ and $SMI\alpha_z$ (Fig. 6) one can see, that the diagnostic performance of both parameters depends only slightly on the amount of thin horizontal rod-like trabecular elements (up to the threshold $\alpha_{th} \approx 1.8$ for *SMI*α and up to the threshold $\alpha_{zth} \approx 2$ for *SMI*α_z value of the r_p stays constantly high), but the underestimation of amount of plates (i.e. taken $\alpha_{th} > 2$) in the structure drastically decrease correlation coefficient. An additional important observation is the increase of the correlation coefficient within the range $2 < \alpha_{zth} < 2.2$ for anisotropic *SMI*α_z (right plot in Fig. 6). This region corresponds to the thin horizontal plates (last row in Fig. 4), which are important for stability of the bone, but do not work as load bearing elements. This means that the best diagnostic performance of the novel morphological parameter SMIα_z is obtained when we separate structure not only according to the morphological form of trabecular elements (plates or rods), but rather according to their mechanical functionality within the structure (bearing of load or support of stability).

3.2 Minkowski Functionals (MF)

Minkowski Functionals (MF) provide a global morphological and topological description of structural properties of multidimensional data (Mecke et al., 1994). According to integral geometry *n*-dimensional body can be completely characterized by *n+1* functionals, which
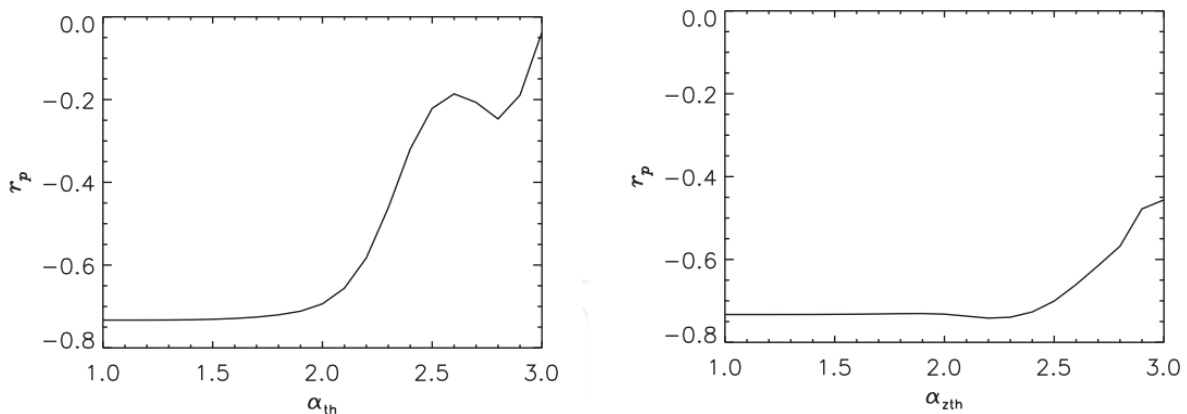
Fig. 6. Pearson's correlation coefficient r_p as a function of threshold value α_{th} for novel combination of *SMI* with isotropic (left) and anisotropic (right) scaling indices.

evaluate both size and shape of the object. In a three-dimensional space they represent the volume (MF_1), surface area (MF_2), integral mean curvature (MF_3) and integral Gaussian curvature (MF_4). Minkowski Functionals are derived from the theory of convex sets and expressed as volume integral for MF_1 and surface integrals over boundary S with principal radii of curvature R_1 and R_2 for other functionals.

$$MF_1(\nu_{th}) = \int_{I(\nu_{th})} dV \, , \qquad MF_3(\nu_{th}) = 1/2 \int_{\partial I(\nu_{th})} (\frac{1}{R_1} + \frac{1}{R_2}) dS$$

$$MF_2(\nu_{th}) = \int_{\partial I(\nu_{th})} dS \, , \qquad MF_4(\nu_{th}) = \int_{\partial I(\nu_{th})} \frac{1}{R_1 R_2} dS \qquad (11)$$

The first two functionals MF_1 and MF_2 describe morphology of the structure and coincide with morphometrical parameters bone volume BV/TV and surface BS/TV fractions. The fourth integral is also known as Euler characteristic χ, which characterises topological connectivity of the structure and can be expressed in terms of Betti numbers β_0 (number of connected components), β_1 (number of tunnels), β_2 (number of cavities):

$$\chi = \beta_0 - \beta_1 + \beta_2 \, . \qquad (12)$$

In the case of binary images we have exactly four global characteristics, which can be used as texture measures for diagnostic of bone strength. For greyscale CT or MR images the bone mineral network must be segmented according to the intensity threshold value ν_{th}. Thus, Minkowski Functionals become a function of an excursion set $I(\nu_{th})$, which is determined by all voxels with $\nu > \nu_{th}$ or $\nu < \nu_{th}$. The calculation of the MF for the binary or images thresholded at a certain threshold ν_{th} can be reduced to the calculation of open vertices (n_v), edges (n_e), faces (n_f) and number of the voxels (n_p), that belong to the excursion set $I(\nu_{th})$ (Michielsen & Raedt, 2001).

$$MF_1(\nu_{th}) = n_p \, , \qquad MF_3(\nu_{th}) = 3n_p - 2n_f + n_e$$

$$MF_2(\nu_{th}) = -6n_p + 2n_f \, , \qquad MF_4(\nu_{th}) = -n_p + n_f - n_e + n_v \qquad (13)$$

In the common approach an excursion set $I(v_{th})$ is defined as the union of image voxels, which have a grey level g below or above a threshold $v_{th} = g_{th}$. Different values of threshold g_{th} describe different tissues of the bone. Scaling Index Method offers a new possibility for binarizing images before calculation of MF (Monetti et al., 2009). Taking a scaling index α_{th} as a threshold variable v_{th} for excursion set I, we compose excursion set $I(\alpha_{th})$ with the structure elements which are selected according to their local topological properties (i.e. rod-like and plate-like substructures). Thus we combine both local and global characteristics and for each Minkowski Functional $MF_{1,2,3,4}$ obtain a new texture measures $MF\alpha_{1,2,3,4}$ and $MF\alpha_{z1,2,3,4}$. In Table 3 we demonstrate diagnostic performance of MF and their combination with isotropic and anisotropic SIM. We compare standard linear multiregression analysis and novel nonlinear combination of global (MF) and local (SIM) topological approaches. One can observe significant improvement of correlation coefficient for the third and the forth Minkowski Functionals (up to the value $r_p = 0.74$), when they are calculated in combination with anisotropic SIM ($MF\alpha_{z3}$ and $MF\alpha_{z4}$). In general nonlinear combination global and local topological characteristics improves correlation with experimental MCS more significantly, than standard linear multiregression analysis. The best correlation with experimental MCS is obtained by choosing substructure with $\alpha_z > 2.8$, what corresponds to thick vertical plate-like trabecular elements (last row in Fig. 5).

Conventional (MF$_{1,2,3,4}$)		0.73	0.6	0.06	0.38
Linear combination of MF with SIM	*isotropic*	0.73	0.65	0.59	0.60
	anisotropic	0.73	0.67	0.62	0.63
Nonlinear combination of MF with SIM	*isotropic (MF$\alpha_{1,2,3,4}$)*	0.71	0.70	0.69	0.47
	anisotropic (MF$\alpha_{z1,2,3,4}$)	0.72	0.73	0.73	0.74

Table 3. Correlation coefficient for conventional Minkowski Functionals (first row), linear combination of MF with isotropic and anisotropic SIM (second row) and novel nonlinear combination of MF with isotropic (*MFα*) and anisotropic (*MFα_z*) SIM (third row).

3.3 Finite Element Method (FEM)

Finite Element Method is the most powerful method in the description of biomechanical behaviour of structures under the external load (Rietbergen et al., 1995). The obvious advantage of the method is that by converting voxels of μCT images into finite element mesh it takes into account exact microarchitecture of the object and thus allows to study both apparent and tissue level biomechanical stresses in structures. In present section we show that the combination of tissue level biomechanical characteristics obtained by FEM with local topological measures calculated by SIM provides complementary understanding of load redistribution between topologically different structure elements. We apply the

linear elastic approach described by generalized Hook's law with the fundamental assumption that deformations are under the yield level. Bone mineral tissue is described as isotropic and elastic material with Young's modulus $Y = 10$ GPa and Poisson's ratio $v = 0.3$. According to the biomechanical experiments we apply Dirichlet boundary conditions to simulate a high friction compressive test in the uniaxial direction (we call it z direction) with constant strain $\varepsilon_z = 1\%$ prescribed on the top surface. As a main mechanical characteristic on tissue level we use the effective strain (Pistoia et al., 2002)

$$\varepsilon_{eff} = \sqrt{2U/Y} \ , \tag{14}$$

which is calculated from the strain energy density

$$U = 1/2\left(\sigma_{xx}\varepsilon_{xx} + \sigma_{yy}\varepsilon_{yy} + \sigma_{zz}\varepsilon_{zz}\right) + \sigma_{xy}\varepsilon_{xy} + \sigma_{xz}\varepsilon_{xz} + \sigma_{yz}\varepsilon_{yz} \tag{15}$$

normalised to Young's modulus Y of the bone mineral material. The energy density U (15) describes the stored energy associated with elastic deformation caused by the external loading. Also linear elastic model is valid only below the yield limit and does not describe development of fractures, the numerically estimated failure load

$$L_{cv} = F_r \cdot k_{cv} \tag{16}$$

is often used as a predictive parameter in correlation analysis with respect to the experimentally measured MCS (Pistoia et al., 2002). We calculate failure load L_{cv} from the apparent total reaction force F_r at the top face A^t

$$F_r = \int \sigma_{zz}^t dA^t \tag{17}$$

by multiplying with a linear scaling factor k_{cv}, which depends on the distribution of the effective strain ε_{eff} in the trabecular bone network

$$k_{cv} = 1 / \sum_{i=1}^{N_{voxels}} H(\varepsilon_{eff} - \varepsilon_{cv}) \ . \tag{18}$$

Here N_{voxels} is number of voxels composing the observed structure and $H(x)$ is Heaviside step function (10). Absolute value of the failure load L_{cv} depends on the critical value of the effective strain ε_{cv}. The best Pearson's correlation coefficient $r_p = 0.76$ with respect to the MCS is obtained for critical value $\varepsilon_{cv} = 0.002$, which takes into account both large and small deformations in the trabecular bone under the vertical load.

We generate a finite element model by converting bone voxels into equally sized and oriented hexahedral elements and calculate effective strain (14) for each voxel of the trabecular structure. Thus SIM and FEM propose alternative representation of the structure on tissue level. Each voxel can be characterised by two new properties: effective strain ε_{eff} obtained by FEM and scaling index α (or α_z) obtained by SIM. Combination of SIM and FEM allows to analyse the redistribution of the deformation energy stored during compressive loading between the trabecular elements with different topological dimensionality. We calculate the average effective strain $<\varepsilon_{eff}>$ for voxels having the same values of scaling indices (Fig. 7). Both in strong and weak bones maximum average effective strain $<\varepsilon_{eff}>$ is accumulated in substructures with $\alpha > 2$ (isotropic SIM) or $\alpha_z \approx 2.5$ (anisotropic SIM), which

corresponds to plate-like trabecular elements, but according to the $P(\alpha)$ spectrum (Fig. 3) the amount of plates in weak bones is smaller than in strong ones. This means that plates along the direction of natural loading are the main load bearing substructure of the trabecular network and the relative amount of vertical plates plays the most important role for bone strength on a global level, while thin horizontal rod and plate structure elements play stabilizing role under different shear loading.
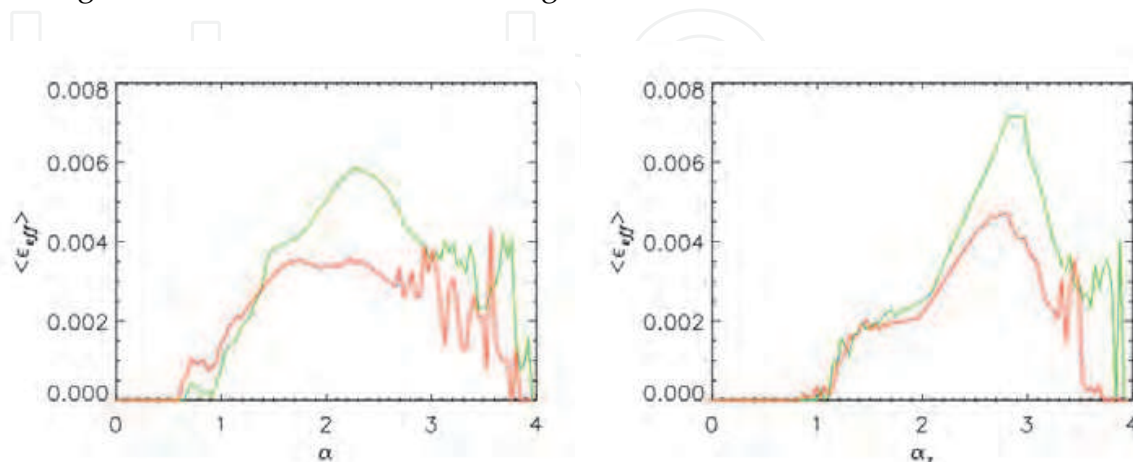

Fig. 7. Effective strain ε_{eff} calculated with FEM averaged over the voxels with the same value of scaling indices calculated with SIM (left: isotropic, right: anisotropic). Red lines: weak bone, green lines: strong bone.

		MF_2	MF_3	MF_4	SMI
Conventional methods		0.60	0.06	0.38	-0.43
Combination with SIM	*isotropic (α)*	0.70	0.69	0.47	-0.73
	anisotropic (α_z)	0.73	0.73	0.74	-0.74

Table 4. Increase of the Pearson's correlation coefficient r_p due to the nonlinear combination with the isotropic (α) and anisotropic (α_z) Scaling Index Method.

	FEM	MF1	$MF\alpha_{z1}$	$MF\alpha_{z2}$	$MF\alpha_{z3}$	$MF\alpha_{z4}$	$SMI\alpha_z$
MCS	0.76	0.73	0.72	0.73	0.73	0.74	-0.74
FEM	1	0.94	0.95	0.94	0.94	0.94	-0.94

Table 5. Pearson's correlation coefficient for the seven strongest numerical methods with respect to the experimental MCS and numerical failure load estimated by FEM.

3.4 Prediction of bone strength with different numerical methods
We assess the diagnostic performance of the numerical methods described in the previous sections by means of correlation analysis with respect to the maximum compressive strength (MCS) experimentally measured in uniaxial compressive test. High values of the Pearson's correlation coefficient r_p are demonstrated only by two texture measures: failure load L_{cv}

estimated by FEM ($r_p = 0.76$) and first Minkowski Functional MF_1, which represents mineral bone volume fraction BV/TV ($r_p = 0.73$). Second Minkowski Functional MF_2, which coincides with bone surface fraction BS/TV and texture measures based on the isotropic and anisotropic Scaling Index Method (Räth et al., 2008) demonstrate only moderate correlation with MCS (*0.6, 0.55* and *0.52* respectively). Morphological parameters, provided by standard software delivered by the μCT scanner manufacture, *Tb.Th.*, *Tb.Sp.*, *Tb.N.* and *SMI*, as well as MF_3 and MF_4 correlate very weak ($r_p < 0.5$) with experiment, but in combination with local topological information provided by isotropic and anisotropic SIM, correlation coefficient significantly increases (Table 4). Thus, we have a group of seven methods (Table 5), which have good diagnostic performance in differentiating between strong and weak trabecular bone structure. They have high Pearson's correlation coefficient with respect to the experimental MCS ($r_p > 0.7$) and correlate very well with the best numerical texture measure, which is failure load estimated by FEM ($r > 0.94$). General feature of these methods is that all of them provide texture measures based both on structure quality and size.

4. Conclusions

Our study clearly shows that in order to give comprehensive description of materials and tissues with porous and irregular structures it is not sufficient to use only global methods. Local topological measures provide complementary information to the global characteristics and their proper evaluation is of a great importance for many scientific purposes. To the best of our knowledge, Scaling Index Method is a unique technique for assessing local topological properties of arbitrary structures. It is well suited for quantifying topological aspects on a local level, especially to discriminate substructures with different dimensionality or separate the inner body and the surface of the object. It can be applied both to greyscale and binary images. By varying the scaling parameter of the method one can characterise the same structure on different levels of dimensionality. SIM provides complementary information to biomechanical (FEM), morphological (SMI) and global topological (MF) methods. Nonlinear combination of SIM with existing numerical techniques improves both qualitative understanding and diagnostic performance of the methods. Calculation of SMI and MF based on the scaling index decomposition of the μCT images of human trabecular bone, which represent a typical example of the biological tissue with irregular structure, significantly improves the correlation with the experimentally measured MCS (Table 4). Comparison on the tissue level of the effective strain calculated by the FEM and scaling indices provided by SIM, shows that the plate-like elements in direction of natural loading are the main load bearing substructure of trabecular network both in strong and weak bones, but the amount of plates in weak bones is reduced in comparison with strong ones, which leads to the global decrease of the bone strength and stability on the global level.

5. Acknowledgments

6. References

Benzi, R.; Paladin, G.; Parisi, G. & Vulpiani, A. (1984). On the multifractal nature of fully developed turbulence and chaotic systems. *J. Phys. A: Math.Gen.*, Vol. 17, pp. 3521-3531

Ding, M. & Hvid, I. (2000). Quantification of age-related changes in the structure mdoel type and trabecular thickness of human tibial cancellous bone. *Bone,* Vol.26, No. 3, pp. 291-295

Grassberger, P.; Badii, R. & Politi, A. (1988). Scaling laws for invariant measures on hyperbolic and nonhyberbolic atractors. *Journal of Statistical Physics,* Vol. 51, No. 1/2, pp. 135-178

Hildebrand, T. & Rüegsegger, P. (1997a). A new method for the model-independent assessment of thickness in three-dimensional images. *J Microsc,* Vol. 185, Pt 1, pp. 67-75

Hildebrand, T. & Rüegsegger, P. (1997b). Quantification of bone microarchitecture with the Structure Model Index. *CMBBE,* Vol.1, pp.15-23

Hildebrand, T.;Laib, A.; Müller, R.; Dequeker, J. & Rüegsegger, P. (1999). Direct three-dimensional morphometric analysis of human cancellous bone: microstructural data from spine, femur iliac crest, and calcaneus. *J Bone Miner Res,* Vol. 14, No. 7, pp.1167-1174

Jensen, M.; Kadanoff, L.P. & Libchaber, A. (1985). Global universality at the onset of chaos: results of a forced Rayleigh-Benard experiment. *Phys. Rev. Lett.* Vol. 55, No. 25, pp. 2798-2801

Kerckhofs, G.; Schrooten, J.; Elicegui, L.; Van Bael, S.; Moesen, M.; Lomov, S. & Wevers, M. (2008). Mechanical characterization of porous structures by the combined use of micro-CT and in-situ loading. *Proceedings of World Conference on Non-Destructive Testing (WCNDT)*, Shanghai, China, 25-28 October 2008

Kerckhofs, G.; Pyka, G.; Loeckx, D.; Van Bael, S.; Schrooten, J. & Wevers, M. (2010). The combined use of micro-CT imaging, in-situ loading and non-rigid image registration for 3D experimental local strain mapping on porous bone tissue engineering scaffolds under compressive loading. *Proceedings of European Conference for non-Destructive Testing (ECNDT)*, Moscow, Russia, 7-11 June 2010

Mecke, K.R.; Buchert, T. & Wagner, H. (1994). Robust morphological measures for large-scale structure in the Universe. *Astron. Astrophys.*, Vol. 288, pp. 697-704

Michielsen, K. & Raedt, H. (2001), Integral-geometry morphological image analysis. *Physics Reports,* Vol.347, pp.461-538

Monetti, R.A.; Boehm, H.; Mueller, D.; Newitt, D.; Majumdar, S.; Rummeny, E.; Link, T.M. & Raeth, C. (2003). Scaling Index Method: a novel nonlinear technique for the analysis of high-resolution MRI of human bones. *Proceedings of Medical Imaging Conference of SPIE,* Vol. 5032, pp. 1777-1786

Monetti, R.A.; Bauer, J.; Mueller, D.; Rummeny, E.; Matsuura, M.; Eckstein, F.; Link, T. & Raeth, C. (2007). Application of the Scaling Index Method to μ-CT images of human trabecular bone for the characterization of biomechanical strength. *Proceedings of Medical Imaging Conference of SPIE,* Vol. 6512, pp. 65124H

Monetti, R.A.; Bauer, J.; Sidorenko, I.; Mueller, D.; Rummeny, E.; Matsuura, M.; Eckstein, F.; Lochmueller, E.M.; Zysset, P. & Raeth, C. (2009). Assessment of the human trabecular bone structure using Minkowski Functionals. *Proceedings of Medical Imaging Conference of SPIE,* Vol. 7262, pp. 7262ON1-7262ON9

Mueller, D.; Link, T.M.; Monetti, R.; Baur, J.; Boehm, H.; Seifert-Klauss, V.; Rummeny, E.J.; Morfill, G.E. & Raeth, C. (2006). The 3D-based scaling index algorithm: a new structure measure to analyze trabecular bone architecture in hifh-resolution MR images in vivo. *Osteoporos. Int.,* Vol. 17, pp. 1783-1493

Paladini, G. & Vulpiani, A. (1987). Anomalous scaling laws in multiftactal objects. *Phys Reports,* Vol. 156, No. 4, pp. 147-225

Pistoia, W.; van Rietbergen, B.; Lochnueller, E.-M.; Lill, C. A.; Eckstein, F. & Ruegsegger, P. (2002). Estimation of distal radius failure load with micro-finite element analysis models based on three-dimensional peripheral quantitative computed tomography images. *Bone,* Vol. 30, No. 6, pp. 842-848

Räth, C. & Morfill, G. (1997). Texture detection and texture duscrimination with anisotropic scaling indices. *J. Opt. Soc. Am. A,* Vol. 14, No. 12, pp. 3208-3215

Räth, C.; Bunk, W.; Huber, M.B.; Morfill, G.E.; Retzlaff, J. & Schuecker, P. (2002). Analysing large-scale structure –I. Weighted scaling indices and constrained randomization. *Mon. Not. R. Astron. Soc.,* Vol. 337, pp. 413-421

Räth, C.; Monetti, R.; Bauer, J.; Sidorenko, I.; Mueller, D.; Matsuura, M.; Lochmueller, E.-M.; Zysset, P. & Eckstein, F. (2008). Strength through structure: visualization and local assessment of the trabecular bone structure. *New Journal of Physics,* Vol. 10, pp. 125010-125027

Rietbergen, B.; Weinans, H.; Huiskes, R. & Odgaard, A. (1995). A new method to determine trabecular bone elastic properties and loading using micromechanical finite-element models. *J. Bioemchanics,* Vol. 28, No. 1, pp. 69-81

Rossmanith, G.; Räth, C.; Banday, A. J. & Morfill, G. (2009). Non-Gaussian signatures in the five-year *WMAP* data as identified with isotropic scaling indices. *MNRAS*, Vol. 399, No. 4, pp.1921–1933
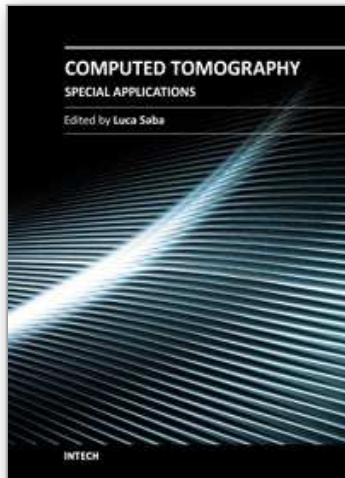
Computed Tomography - Special Applications

Edited by Dr. Luca Saba

CT has evolved into an indispensable imaging method in clinical routine. The first generation of CT scanners developed in the 1970s and numerous innovations have improved the utility and application field of the CT, such as the introduction of helical systems that allowed the development of the "volumetric CT" concept. Recently interesting technical, anthropomorphic, forensic and archeological as well as paleontological applications of computed tomography have been developed. These applications further strengthen the method as a generic diagnostic tool for non destructive material testing and three dimensional visualization beyond its medical use.

How to reference

In order to correctly reference this scholarly work, feel free to copy and paste the following:

INTECH
open science | open minds